Article

Engineering of Nanostructured Carbon Catalyst Supports for the Continuous Reduction of Bromate in Drinking Water

João M. Cunha Bessa da Costa [1,2], José R. Monteiro Barbosa [1,2], João Restivo [1,2,*], Carla A. Orge [1,2], Anabela Nogueira [3], Sérgio Castro-Silva [3], Manuel F. Ribeiro Pereira [1,2] and Olívia S. Gonçalves Pinto Soares [1,2,*]

[1] LSRE-LCM—Laboratory of Separation and Reaction Engineering-Laboratory of Catalysis and Materials, Faculty of Engineering, University of Porto, Rua Dr. Roberto Frias, 4200-465 Porto, Portugal; jmcbcosta@fe.up.pt (J.M.C.B.d.C.); jrbarbosa@fe.up.pt (J.R.M.B.); carlaorge@fe.up.pt (C.A.O.); fpereira@fe.up.pt (M.F.R.P.)

[2] ALiCE—Associate Laboratory in Chemical Engineering, Faculty of Engineering, University of Porto, Rua Dr. Roberto Frias, 4200-465 Porto, Portugal

[3] Adventech—Advanced Environmental Technologies Lda., Centro Empresarial e Tecnológico, Rua de Fundões, 151, 3700-121 São João da Madeira, Portugal; anabela.nogueira@adventech.pt (A.N.); sergio.silva@adventech.pt (S.C.-S.)

* Correspondence: jrestivo@fe.up.pt (J.R.); salome.soares@fe.up.pt (O.S.G.P.S.)

Abstract: Recent works in the development of nanostructured catalysts for bromate reduction in drinking water under hydrogen have highlighted the importance of the properties of the metallic phase support in their overall performance. Since most works in catalyst development are carried out in powder form, there is an overlooked gap in the correlation between catalyst support properties and performance in typical continuous applications such as fixed bed reactors. In this work, it is shown that the mechanical modification of commercially available carbon nanotubes, one of the most promising supports, can significantly enhance the activity of the catalytic system when tested in a stirred tank reactor, but upon transition to a fixed bed reactor, the formation of preferential pathways for the liquid flow and high pressure drops were observed. This effect could be minimized by the addition of an inert filler to increase the bed porosity; however, the improvement in catalytic performance when compared with the as-received support material was not retained. The operation of the continuous catalytic system was then optimized using a 1 wt.% Pd catalyst supported on the as-received carbon nanotubes. Effluent and hydrogen flow rates as well as catalyst loadings were systematically optimized to find an efficient set of parameters for the operation of the system, regarding its catalytic performance, capacity to treat large effluent flows, and minimization of catalyst and hydrogen requirements. Experiments carried out in the presence of distilled water as a reaction medium demonstrate that bromate can be efficiently removed from the liquid phase, whereas when using a real water matrix, a tendency for the deactivation of the catalyst over time was more apparent throughout 200 flow passages over the catalytic bed, which was mostly attributed to the competitive adsorption of inorganic matter on the catalyst active centers, or the formation of mineral deposits blocking access to the catalyst.

Keywords: catalytic reduction with hydrogen; bromate reduction; nanostructured catalysts; carbon nanotubes

1. Introduction

Safe drinking water is a basic human right and a precondition for public health and development [1]. Bromate is highly soluble, stable in water, and difficult to remove using conventional treatment technologies [2]. It is not usually present in drinking water, but it can occur as a result of pollution from industrial sources and sometimes as a consequence of its presence in contaminated soil. However, the main reason for its occurrence in drinking

water is its formation during ozonation, being commonly associated with disinfection as a by-product formed during treatment [1,2]. Treatment processes where bromate can form as a disinfection by-product (DBP) include ozonation followed by hypochlorination and/or chloramination, and hypochlorination alone [2]. Its occurrence has been reported in drinking-water at concentrations ranging from less than 2, to 293 μg L^{-1}, depending on the bromide ion concentration, ozone dosage, pH, alkalinity, and dissolved organic carbon [1].

Data regarding long-term exposure to bromate in drinking water and associated dangers is very limited. Symptoms due to acute accidental poisoning include several gastrointestinal irritations, central nervous system depression, and renal failure. The kidneys are the biggest target for cancer and its toxicity, with other risks including low sperm counts and the possibility of thyroid and peritoneum cancer [2,3]. Based on its toxic effects, the International Agency for Research on Cancer (IARC) has classified bromate as possibly carcinogenic to humans, and the World Health Organization (WHO) has established a maximum value of 10 μg L^{-1} as a guideline value for bromate in drinking water [1]. With this classification by the IARC and with the objective to obtain safe drinking water, there has been an increasing interest in developing technologies for bromate removal from water.

Different approaches have been attempted to remove or control the presence of bromate ions in water, such as the minimization of its formation during the ozonation or their removal from contaminated water. Out of the latter, various methods are available, namely: photocatalysis [4], adsorption [3], ion exchange [5], electrochemical reduction [6], and heterogeneous catalysis under hydrogen [7]. Out of these, the heterogeneous catalytic reduction with hydrogen over supported metal catalysts is one of the most promising processes, having shown high removal efficiency and no production of unwanted sludges [7]. The reduction of bromate by hydrogen can occur by different pathways; in which the most relevant is the adsorption of the bromate ion on the catalyst surface and its reduction by the adsorbed and dissociated hydrogen [7].

It has been demonstrated that different metals (Pt, Pd, Cu, Sn, Rh, Ru, Ni, Ir, Fe, and Zn) supported on activated carbon (AC) are active for the catalytic reduction of bromate with hydrogen at ambient temperature and pressure, with the noble metals Ru, Pd, Pt, and Rh showing the most promising results [7]. Out of these metals, Pd has been identified as the most promising [7,8].

The support of the metal phase can influence the density, size, and morphology of the active centres of the metal and, as a result, the activity of the catalyst. Different supports such as AC, multi-walled carbon nanotubes (MWCNT), and titanium dioxide (TiO$_2$) were reported [8–10] as supports for the metal phase, having shown that the interaction of the support with the metallic phase is responsible for substantial differences in activity. In general, distinct catalytic performances were reported when using catalysts with similar metallic loadings but supported on different materials. These differences were attributed to the different properties of the supports, namely the surface charge, the porous structure, and the interaction of the metal with the support [11]. The use of carbon nanotubes (CNT) as supports has shown very promising results for the catalytic reduction of bromate, allowing the reduction of bromate to bromide, in contrast to the results obtained when AC is used as a support, where high adsorption of bromate is observed [9]. Soares et al. [9] has reported that the supports play an important role in bromate reduction under hydrogen in water, highlighting the excellent effect of N-doping. Doping CNT with nitrogen can result in outstanding performances due to the distribution and arrangement of the heteroatoms in the CNT structure, providing additional electrons for the graphitic lattice. Furthermore, reduction of CNT entanglement by applying a ball-milling treatment was also verified to be a promising way to improve the catalytic activity of the supported Pd catalysts. This allows to modify the length of the nanotubes and permits the opening of the closed ends, thus increasing the surface area and providing higher accessibility of the ionic species in water to the support surface [9,12].

The majority of works available regarding catalytic bromate reduction in water focus on the development and/or testing of catalysts and reaction conditions using powder materials in stirred tank reactors [9–11,13–15]. Only few works have been carried out in continuous reactors, mainly using macro-structured supports coated with the active phase deposited on activated carbon fibres or felts [16–18]. The same is true for other catalytic reduction reactions such as nitrate or nitrite reduction [19–22].

This work aims to provide insights on the transition from batch stirred tank reactors to a continuous system towards the design of a nanostructured catalytic system for the efficient reduction of bromate from drinking water at environmentally relevant levels (i.e., micrograms per litre). For this end, using palladium-based nanostructured catalysts, a systematic comparison between supports with different chemical and textural properties for the metal phase was carried out using a stirred tank reactor. Multi-walled carbon nanotubes were used as the base of the supports and subjected to different physical and/or chemical treatments, resulting in different properties. The best performing catalysts were selected for testing in a lab-scale fixed bed continuous reactor pilot unit, evaluating the capability of the catalysts to achieve contamination levels below those in the relevant legislations or recommended by the authorities when used in practical conditions. Effluent and hydrogen flow rates, as well as catalyst loadings were systematically optimized to find an efficient set of parameters for the operation of the system, regarding its catalytic performance, capacity to treat large effluent flows, and minimization of catalyst and hydrogen requirements. Moreover, long-term operation of the unit was performed using real water from a water treatment plant (WTP) from Coimbra, Portugal, to assess the stability of the catalysts over longer reaction times and ensure their potential for practical applications.

2. Materials and Methods

2.1. Supports Preparation

A series of nanostructured supports were prepared to provide insight into the role of the support properties in the catalytic activity of the metallic phase, and in the behavior of the fixed bed reactor. Multi-walled carbon nanotubes of 90% + purity (MWCNT-O, from Nanocyl, Sambreville, Belgium, NC7000) were used as-received and after modification of their surface chemical and textural properties. Oxygen-containing surface functionalities were introduced by treatment with boiling nitric acid using a widely reported procedure (MWCNT-HNO$_3$) [9,23]. The acid treated MWCNT were then thermally treated at 900 °C under N$_2$, which has previously been shown to remove the acidic oxygen-containing surface functionalities, while retaining the structural defects introduced during the acid treatment (MWCNT-HNO$_3$-900) [9]. The as-received MWCNT were also mechanically modified by ball-milling to promote the disentanglement and breaking of the nanotubes, resulting in a sample with a higher specific surface area, smaller particle diameter, and open-ended tubes (MWCNT-BM) [9,12]. Finally, nitrogen doping was achieved using a mechano-thermal approach, where melamine, as a nitrogen precursor, was introduced during ball-milling of the as-received MWCNT, and the resulting mixture was thermally treated under N$_2$ at 600 °C to achieve decomposition of the melamine (MWCNT@N) [24]. A commercial activated carbon support was also used for comparison purposes as an example of a traditional catalyst support (AC).

2.2. Catalysts Preparation

The nanostructured metallic catalysts were prepared by incipient wetness impregnation using an aqueous solution from the corresponding metal salt (PdCl$_2$), using the supports described in Section 2.1. The amount of metal in each catalyst was maintained constant at 1 wt.%. Impregnation was carried out under ultrasonic mixing and the precursor solution was added dropwise to the supports using a peristaltic pump. The obtained mixture was left under ultrasonic mixing at room temperature for 90 min and the samples were left to dry at 100 °C overnight. After impregnation, the catalysts were thermally

treated under a flow of N_2 at 200 °C for 1 h and then reduced under a flow of H_2 at 200 °C for 3 h.

2.3. Materials Characterization

Catalyst supports prepared by the same methodologies as used in this work have been extensively characterized elsewhere [9,25]. The textural properties of the catalysts were obtained by the analysis of N_2 isothermal adsorption curves at −196 °C measured using a QuantaChrome Nova 4200e instrument. The specific surface area was derived from the data using the Brunauer–Emmett–Teller method (S_{BET}), and elemental analysis (EA) was used to quantify carbon, nitrogen, hydrogen, sulfur, and oxygen content using a MICRO and an OXY cube analyser from Elemental GmbH. Thermogravimetric analyses (TGA) were carried out using an STA 409 PC/4/H Luxx Netzsch thermal analyser to obtain moisture, volatile, fixed carbon, and ashes content of the supports.

2.4. Catalytic Experiments

The catalysts were tested in semi-batch and continuous mode. The semi-batch experiments were carried out in a custom-designed semi-batch tank reactor equipped with a magnetic stirrer for a total reaction time of 3 h, using hydrogen as a reducing agent. Then, 100 mg of catalyst were used in 800 mL of bromate solution for a 0.125 g L^{-1} catalyst loading. Hydrogen flow was kept at 50 cm^3 min^{-1} and the catalyst suspension was maintained under constant stirring at 400 rpm.

A pre-reduction/saturation step was used where the 100 mg of catalyst were added to 790 mL of distilled water and stirred under flowing hydrogen for 15 min. After this period, 10 mL of a concentrated bromate solution was added to the reactor to achieve an initial concentration of 200 ppb. The initial reaction time was marked when the first sample was collected from the reactor after injection of the concentrated solution. Catalysts were recovered after reaction by filtration and dried under air overnight.

The continuous reactions were initially carried out with a 5 mL min^{-1} feed flow of water containing a concentration of 200 ppb of bromate in a fixed bed tube reactor (Figure 1). The system used consisted of two columns; one was used to saturate the solution with hydrogen, where a flow rate of 50 cm^3 min^{-1} was maintained throughout the reaction. The solution was subsequently circulated with a peristaltic pump to the other column, in which 200 mg of the selected catalyst was located. All the experiments were carried out at room temperature and atmospheric pressure. Later, experiments were carried out with varying operation conditions, towards the optimization of the continuous catalytic system. The bromate reduction progress was followed using a Shimadzu Bromate Analysis LC system, using a 12 mM $NaHCO_3$ and 0.6 mM Na_2CO_3 mobile phase for bromate separation, and a 1.5 M KBr, 1.0 M H_2SO_4, and 1.2 mM $NaNO_2$ solution for post-column reaction for UV detection at 256 nm.

Bromate removal was evaluated using different types of water: Distilled water, groundwater from a well (Coimbra, Portugal), and water from a water treatment plant (WTP) (Coimbra, Portugal). The characteristics of the real waters obtained are listed in Table 1.

The leaching of metals from the catalysts after the reactions was evaluated by ICP-OES ICAP 7400 THERMO (inductively coupled plasma optical emission spectrometry).
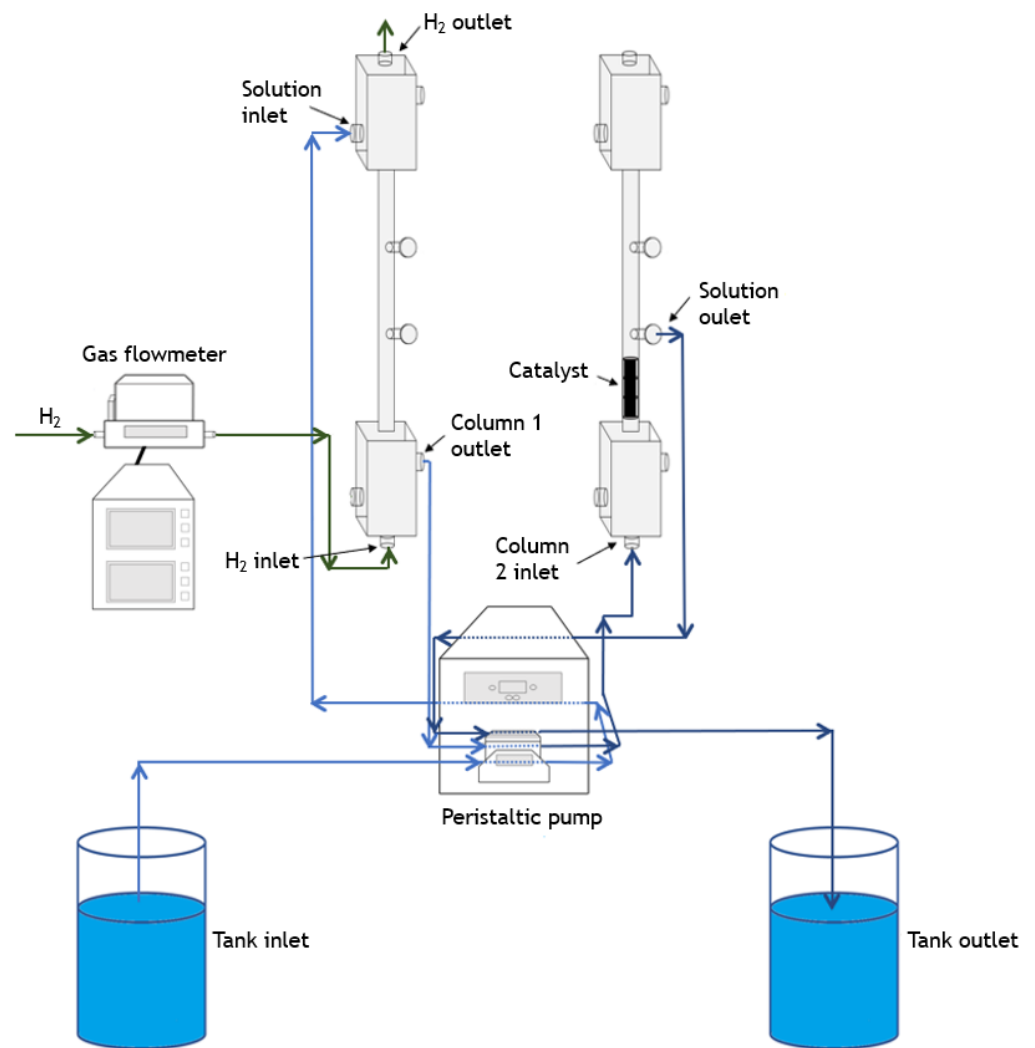
Figure 1. Schematic representation of the reactor system used for reduction of bromate in continuous mode.

Table 1. Characteristics of groundwater obtained from a well and from a WTP in Coimbra, Portugal.

	"Well"	"WTP"
pH	6.59	6.62
Conductivity (μS cm^{-1})	423	416
TOC (mg L^{-1})	3.6	3.7
TC (mg L^{-1})	40.8	39.9
IC (mg L^{-1})	37.1	36.1
BrO$_3^-$ (mg L^{-1})	-	-
Br$^-$ (mg L^{-1})	0.32	5.33
NO$_3^-$ (mg L^{-1})	1.30	0.33
NO$_2^-$ (mg L^{-1})	0.07	-
Cl$^-$ (mg L^{-1})	5.16	0.42
SO$_4^{2-}$ (mg L^{-1})	0.17	-
Na$^+$ (mg L^{-1})	7.17	0.10
NH$_4^+$ (mg L^{-1})	1.11	0.63
Ca^{2+} (mg L^{-1})	17.7	1.35
Mg^{2+} (mg L^{-1})	3.35	-

3. Results and Discussion

3.1. Materials Characterization

N_2 isothermal adsorption-desorption at -196 °C were performed to evaluate the textural modifications induced by the different treatments applied to the supports. Table 2 shows the textural properties of the as-received and modified MWCNT supports and respective nanocatalysts.

Table 2. Relevant textural and chemical properties of the selected carbon supports and respective nanocatalysts.

Support (Catalyst)	S_{BET} (± 5 m^2 g^{-1})	S_{MESO} (± 5 m^2 g^{-1})	$V_{P,P/P0=0.95}$ (± 0.005 cm^3 g^{-1})	V_{MICRO} (± 0.005 cm^3 g^{-1})
AC	897	117	0.455	0.321
(1% Pd/AC)	(855)	(120)	(0.442)	(0.303)
MWCNT-O	255		0.498	
(1% Pd/MWCNT-O)	(201)	-	(0.475)	-
MWCNT-BM	318		0.569	
(1% Pd/MWCNT-BM)	(227)	-	(0.428)	-
MWCNT@N	225		0.494	
(1% Pd/MWCNT@N)	(177)	-	(0.401)	-
MWCNT-HNO$_3$	310		0.695	
(1% Pd/MWCNT-HNO$_3$)	(263)	-	(0.557)	-
MWCNT-HNO$_3$-900	316		0.653	
(1% Pd/MWCNT-HNO$_3$-900)	(328)	-	(0.727)	-

The modification of the textural properties of the as-received MWCNT (MWCNT-O) during the processes described in this work are well known and widely reported [12,26,27]. In short, ball-milling (MWCNT-BM) led to an increase in the specific surface area from 255 m^2 g^{-1} to 318 m^2 g^{-1} attributed to the disentanglement of MWCNT bundles as well as the shortening of the tubes and opening of tube ends [12]. On the other hand, the inclusion of a nitrogen precursor during milling (MWCNT@N) decreased the value of S_{BET} due to the blocking of the pores by nitrogen surface groups [25]. The nitric acid oxidation of MWCNT (MWCNT-HNO$_3$) is also well known to increase the specific surface area. It resulted in an increase of the specific surface area from 255 m^2 g^{-1} to 310 m^2 g^{-1} due to the opening of tube ends and the introduction of structural defects on sidewalls, both directly impacting the textural properties [23,28]. This was retained after thermal treatment of the MWCNT (MWCNT-HNO$_3$-900). Furthermore, nitric acid oxidative treatment also leads to the disentanglement of MWCNT bundles and shortening of MWCNT length [29,30], which resulted in an increase in total pore volume from 0.498 cm^3 g^{-1} to 0.695 cm^3 g^{-1}. A decrease in the surface area and pore volume of the supports upon impregnation with the metallic phases was observed, which is consistent with some blockage of the pore structure or cavities of both AC and MWCNT.

The elemental composition of the catalyst supports was determined by CNHSO analysis, as shown in Table 3.

Table 3. Elemental analysis of selected carbon supports.

Sample	Carbon (%m/m)	Hydrogen (%m/m)	Nitrogen (%m/m)	Sulfur (%m/m)	Oxygen (%m/m)
AC	84.6	0.86	0.01	0.67	5.90
MWCNT-O	88.4	0.25	0.00	0.00	1.10
MWCNT@N	83.1	0.39	4.90	0.00	2.20
MWCNT-HNO$_3$	87.9	0.35	0.01	0.00	5.10
MWCNT-HNO$_3$-900	95.9	0.20	0.01	0.00	0.66

The MWCNT-O sample presented ~90% carbon weight fraction, which is consistent with the manufacturer's specifications. The AC carbon weight fraction was also in accordance with the manufacturer's specifications (~84% carbon and 6% oxygen). The nitrogen doping procedure allowed for the incorporation of 4.9% of nitrogen and increased the oxygen content, confirming the successful doping of the catalyst support. Likewise, nitric acid oxidation increased oxygen content to 5.1%, which was mostly removed by thermally treating the support at 900 °C under an inert atmosphere. The ball-milling of the MWCNT is already well known to not change the elemental composition of the materials [12].

3.2. Catalytic Experiments

Monometallic 1 wt.% Pd catalysts were tested for their ability to reduce bromate in water. Initially, the effect of each support was analyzed in a semi-batch reactor system, and then the best performing supports were selected and tested using a continuous system towards obtaining an optimized catalytic system for bromate reduction in water.

3.2.1. Bromate Catalytic Reduction in a Semi-Batch Reactor

Figure 2 presents the performance of the monometallic 1 wt.% Pd catalysts during bromate reduction under hydrogen, supported on as-received and modified nanostructured carbon supports. The catalytic performance of the monometallic catalyst supported on activated carbon is included for reference as well as a blank test using only hydrogen to evaluate the role of the reducing agent.
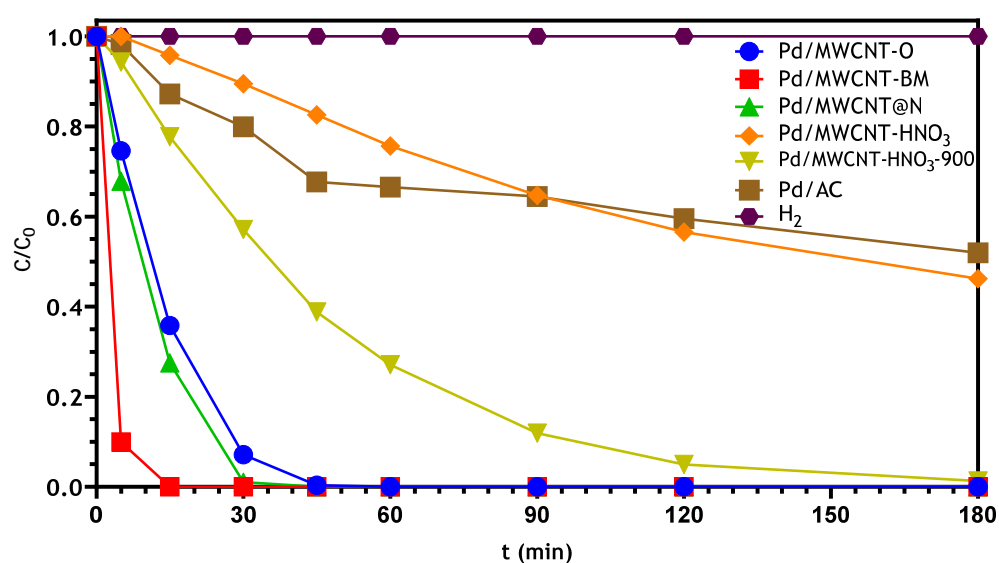

Figure 2. Dimensionless bromate concentration during semi-batch hydrogen reduction over 1 wt.% Pd catalysts on different carbon supports. ($H_2 = 50$ cm^3 min^{-1}, C_0 (BrO$_3^-$) = 200 ppb, 0.125 g_{CAT} L^{-1}).

It is clear from Figure 2 that the nature of the support used for the metallic phase has a substantial impact on the performance of the catalyst. When only hydrogen is used, no removal of bromate was observed during 3 h of reaction, suggesting that without the presence of the catalyst, the activation of hydrogen molecules does not occur under tested experimental conditions. Comparing the bromate reduction achieved by the two as-received supports (MWCNT-O and AC) confirms that, even at the ug L^{-1} level, the nanostructured MWCNT support is much more active than the AC support for the same metallic phase. These had previously been reported at the mg L^{-1} level and attributed to a combination of the reduced impact of diffusional limitations due to the mesoporous nature of the MWCNT entanglements (when compared with the microporous AC) and the contribution of the adsorption of bromate on the graphitic support and reaction with spilled-over hydrogen [16]. On a similar note, the acid treated MWCNT were found to have the

worst catalytic performance of the nanostructured carbon supports. It has been previously shown that acidic carbon surfaces have a negative impact in liquid phase hydrogenation of oxyanions [9,31]. The acidic treatment of the MWCNT increased the specific surface area. Thus, the surface chemistry of the support rather than the textural properties is responsible for the loss of activity. This is further shown by the improvement in performance when the acid treated support was heat treated at 900 °C under nitrogen (MWCNT-HNO$_3$-900), for which some of the original support activity was recovered. The presence of oxygenated surface groups, which may act as anchoring points for the metallic particles, is known to influence the dispersion of the impregnated metal; however, PdCl$_2$ (the precursor used in this work for catalyst synthesis) is known to have a preference for protonated surface groups [32]. On the other hand, surface oxygen is known to interfere with the Pd and carbon surface interaction taking place through a π-electron donation-reception mechanism, which is responsible for Pd dispersion, resulting in poor dispersion on carbon surfaces with high oxygen content [33]. This was also found for carbon surfaces with very high surface oxygen content, where interactions between the Pd precursor and acidic oxide groups can quickly reduce the metal and form large particles [34,35]. The recovery of activity found for the MWCNT-HNO$_3$-900 support is then explained by the removal of oxygenated surface functionalities during thermal treatment. Nevertheless, the catalyst does not reach the levels of activity of the original support even though the surface chemistry is known to be similar [23]. This is contrary to what has been observed with 95%+ purity MWCNT from the same supplier at higher initial bromate concentration, where the activity of as-received and heat-treated samples was very similar [9]. Several phenomena are likely taking place that result in this loss of activity. Acid treatments are known to introduce defects on MWCNT [34], which in turn can affect both dispersion and the support-metal electronic interaction [36]. High temperature calcination is known to, on the other hand, lead to the transition of defective graphitic carbon to ordered supports [36]. Acid treatment (boiling or otherwise) is also used for the purification of MWCNT to remove metallic impurities, in particular those used for catalytic growth of the nanotubes, which may also present activity as hydrogenation catalysts [37]. Moreover, thermal treatment is also known to degrade amorphous carbon that may form during the growth of the nanotubes, which can possibly form sites for Pd dispersion [37]. Thus, even if the acid treatment and removal of oxygenated surface groups could result in a support with similar or even improved performance as the as-received MWCNT, the combination of thermal transformation of defects into ordered carbon, and the purification of the MWCNT during acid treatment are likely resulting in a reduced activity for the MWCNT-HNO$_3$-900 sample.

The mechanical modification of the as-received MWCNT (MWCNT-BM) resulted in a Pd catalyst with increased activity during bromate hydrogenation. Again, the specific surface area of the carbon nanotubes suffered an increase during their modification due to disentanglement, breaking, and opening to end-tips, while no changes in surface chemistry are expected [12]. Thus, the textural properties of the ball-milled support have a more noticeable role than in the acid treated samples. Nevertheless, an additional effect must be present as S$_{BET}$ for MWCNT-BM is very similar to that measured for MWCNT-HNO$_3$-900, which has been proposed to be directly correlated with the disentanglement of the nanotubes during milling, which occurs to a lesser extent during acid and thermal treatments of the as-received MWCNT, leading to easier diffusion of reactants [9,38]. Ball-milling has also been shown to increase the defect density in carbon nanotubes as the sp^2 structure is disrupted [39]. The length of the tubes has also been proposed to influence the dispersion of a metallic phase by facilitating, in longer tubes, the formation of larger particles by diffusion of metallic atoms on the carbon surface, which would be hindered in the smaller ball-milled MWCNT [39]. The combination of these factors leads to the high activity of the MWCNT-BM supported catalyst. Interestingly, and contrary to what has been seen in a previous work carried out with 95%+ purity MWCNT in the ppm bromate concentration range [9], the doping of MWCNT with nitrogen by dry ball-milling and thermal treatment (MWCNT@N) resulted in a catalyst with worse performance than the simply ball-milled

sample. In fact, only a small improvement was found when compared with the as-received support. Textural characterization of both as-received samples shows an increase in S_{BET} and V_p for the 90%+ purity MWCNT (175 to 255 $m^2\ g^{-1}$, and 0.392 to 0.498 $m^2\ g^{-1}$, for 95% and 90%, respectively). Several factors influencing MWCNT surface area are discussed in the literature, and in general it is expected that higher purity products have higher surface area. However, an increase in specific surface area for a lower purity product is not unseen, and several aspects of the synthesis could contribute to this increase, including the use of a high surface area growth catalyst, or a decrease in surface area due to MWCNT damage during acid purification or the graphitization of the carbon nanotubes during synthesis with the removal of structural defects [26]. The differences in the textural properties resulted in a slightly lower amount of nitrogen introduced (4.9 vs. 5.1 wt.%), and a decrease in specific surface area that was not seen in previously reported works [9,24,25,27,40]. Thus, even if the basic nature of nitrogen-doped carbon is known to induce an increase in the catalytic activity of supported Pd in bromate hydrogenation [9], the decrease in the specific surface area negatively affected the catalytic performance.

3.2.2. Bromate Catalytic Reduction in a Continuous Reactor

To examine their potential for industrial applications, continuous catalytic bromate reduction experiments were conducted in a fixed bed tube reactor in which the three best catalysts obtained during the semi-batch experiments were tested (1 wt.% Pd/MWCNT-O, 1 wt.% Pd/MWCNT@N, and 1 wt.% Pd/MWCNT-BM). In technical applications using conventional powder catalysts in continuous fixed bed systems, difficulties associated with high pressure drops and poor bed flow distributions are usually reported [41]. The latter, in the case of the present work, resulted in inconsistent results and catalytic performances worse than expected. At first, the catalytic reduction of bromate was carried out using 200 mg of the selected catalyst in the fixed bed. Using the ball-milled sample, extremely high bed compaction was observed, which prevented the passage of the solution in the column where the catalyst was located. After encountering this problem, the catalyst loading was reduced to 100 mg; however, the catalytic results for this sample were very irregular, confirming a weak dispersion in the reactor, poor radial distribution of the solution flow, and possibly its passage through preferential paths. It is important to highlight that only liquid was passing through the bed since it was used a system with two columns; therefore, these problems cannot be attributed to the entrainment by the gas. It has been reported that capillary forces predominate over viscous and gravitational forces for catalyst particles below a certain limit (depending on the nature of the phases and the reactor configuration) and there is a tendency for the formation of preferential pathways leading to poor radial dispersion [42]. Silicon carbide (carborundum) with a particle size of 0.500 mm in a proportion of 2/3 was added to the catalytic bed, which allowed the creation of porosity, helping with radial dispersion. Figure 3 presents the performance of the monometallic 1 wt.% Pd catalysts with the addition of carborundum during the continuous bromate reduction. Under these conditions, the catalysts performance was enhanced, whereupon the Pd catalyst supported on the original multi-walled carbon nanotubes (MWCNT-O) showed to be the most promising, resulting in outlet bromate concentrations significantly below the legal limit of 10 $\mu g\ L^{-1}$ throughout the entire duration of the reaction, with bromate conversion rates of more than 99%. In fact, for this catalyst, after 8 h of reaction time (~50 flow passages through the bed), an outlet concentration of bromate of about ~1 $\mu g\ L^{-1}$ was obtained. These results differ from those obtained in the semi-batch reactor where the sample with the best results was the MWCNT-BM followed by the MWCNT@N and finally the MWCNT-O (see Section 3.2.1). Even after using 0.500 mm carborundum, the milled samples showed greater compaction, introducing transport limitations and/or poor flow distributions. Smaller particles, which are the case for these milled samples, are intrinsically linked to high capillary forces, which result in poor radial dispersion in the reactor [42]. The milling of carbon nanotubes has been shown to reduce its mean particle size due to the disentanglement of agglomerates [12]. Thus, even when using an inert filler,

the mean particle size of the catalyst bed with the milled catalyst supports will be shifted to smaller sizes and smaller bed voidages, resulting in more predominant viscous forces and the formation of preferential pathways through the catalytic bed [42].
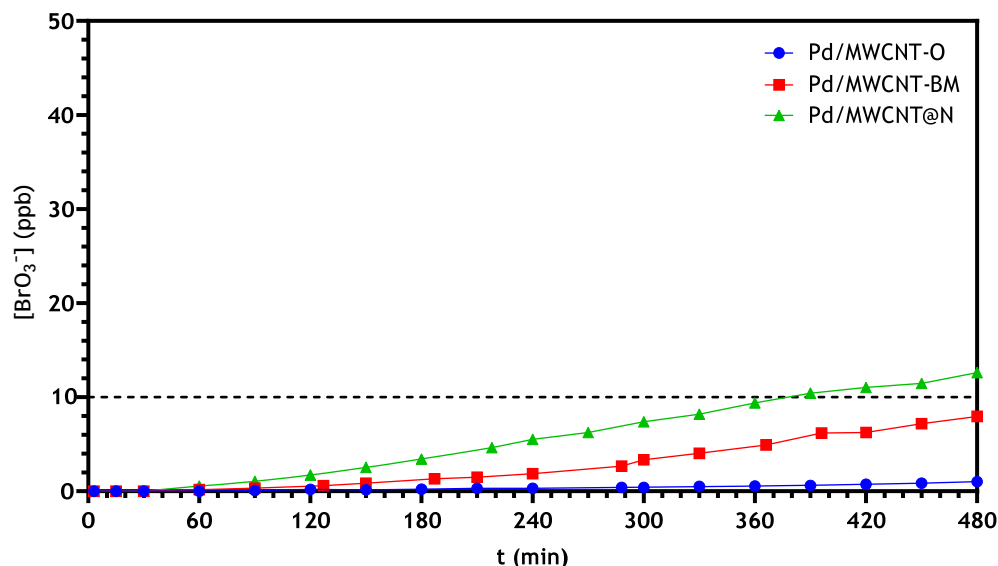

Figure 3. Bromate concentration (ppb) during continuous hydrogen reduction over the catalysts 1 wt.% Pd/MWCNT-O, 1 wt.% Pd/MWCNT@N and 1 wt.% Pd/MWCNT-BM mixed with 0.500 mm carborundum under H_2. ($Q = 5$ mL min^{-1}, 200 mg$_{CAT}$, $H_2 = 50$ cm^3 min^{-1}, C (BrO$_3^-$) = 200 ppb).

In any case, these results show that the performance of the system can be immensely improved by increasing radial dispersion with the dilution of the catalyst with inert particles, which was more evident for the smaller particle sizes (milled samples). All three catalysts showed more than 93% bromate conversion rates during the 8 h of reaction time. This is in line with most reports for continuous bromate reduction, mostly carried out on the milligram per liter level [16,18,43]. Even so, it is worth noting the tendency for a slight deactivation of the catalysts over time, which can be more apparent towards the end of the reactions. Dissolution of metals could be a serious problem in practical uses; thus, the metal content in the treated solution was analyzed to assess the leaching of the catalysts and somewhat verify their physical stability. These analyses were performed by ICP-OES in the post-reaction solutions for each catalyst used and the percentages of leached metals showed to be below 0.30% for all, ranging from ~0.16% to ~0.28%, which can be considered insignificant. This suggests that the catalysts had a good stability in the packed bed mode and could be effective for longer reaction times. The same kind of results regarding palladium leaching were reported, where the amounts of leached palladium are below the detection limits in some cases [44,45], or considered negligible in others (<0.001 wt.% Pd) [38,46].

3.2.3. Optimization of Continuous Reactor Operating Conditions

As assessed before, the support for the metal phase has a significant impact on the catalyst activity, in which the physical and chemical properties of the materials play a significant role in the catalytic reaction. Still, the system and the conditions used for the reactions can be equally important to be able to successfully reduce bromate at maximum efficiency. It has been previously shown that catalyst dilution with inert particles can immensely help improve the performance of the reactor; furthermore, based on the previous experimental results, with the aim to maximize reactor efficiency, the parameters regarding gas flow rate, feed flow rate, and catalyst loading were subjected to varied conditions to find the optimal operation conditions. The 1 wt.% Pd/MWCNT-O was used for the assessment of the optimal conditions. On a first step, different H_2 flow rates were

tested (5, 12.5, 25, 50, and 75 cm^3 min^{-1}) and the results obtained in these experiments are presented in Figure 4.
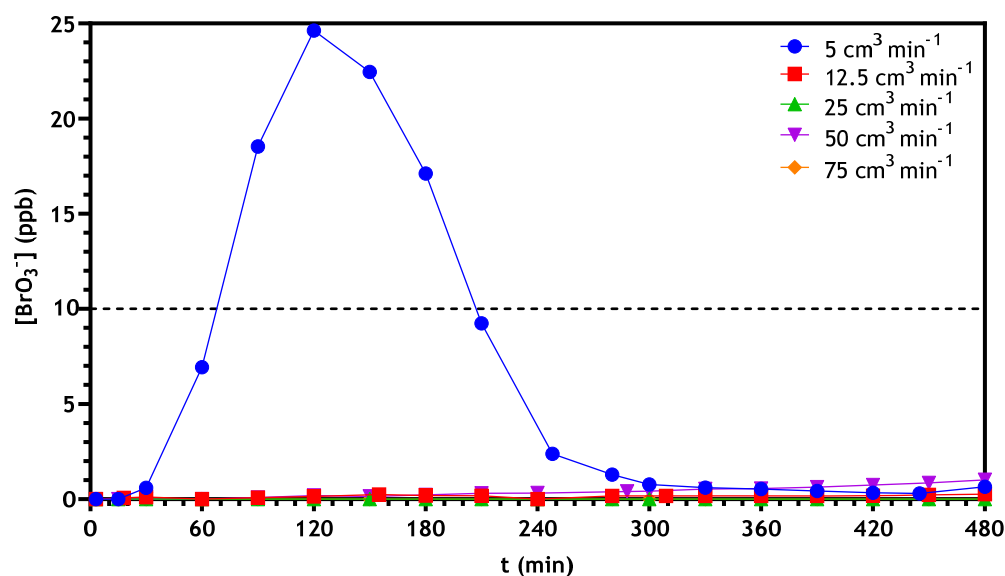

Figure 4. Bromate concentration (ppb) during continuous hydrogen reduction over the catalyst 1 wt.% Pd/MWCNT-O mixed with 0.500 mm carborundum under different H$_2$ flow rates. (Q = 5 mL min^{-1}, 200 mg$_{CAT}$, C (BrO$_3{}^-$) = 200 ppb).

From these results, it can be seen that every gas flow rate resulted in similar conversion profiles, except the 5 cm^3 min^{-1}. As it is suggested in the literature, the reaction mechanism involves the dissociative adsorption of hydrogen on the surface of the metal catalyst, and the reaction between adsorbed bromate ion and the hydrogen atoms [7]; hence, the determination of the optimal hydrogen flow rate is a very important step. From the results obtained, an increase in the H$_2$ flow above 12.5 cm^3 min^{-1} allows no better bromate reduction than higher flow rates, confirming that the solution could be saturated with hydrogen using this value. Regarding the use of 5 cm^3 min^{-1} of H$_2$, it is likely that it takes more time for the solution to be fully saturated with hydrogen, resulting in a delay in the activation of the catalyst during this experiment. Once the solution was fully saturated with hydrogen, the catalyst activity was restored and outlet bromate concentrations were once again very low, in pair with the other experiments. Soares et al. [47] reported a delay in semi-batch NO$_3{}^-$ reduction when using an unsaturated solution when compared with a pre-saturated solution. This was explained by the time necessary to reduce the metal with hydrogen and that its presence in water allows a rearrangement of the metal phase.

Furthermore, it can be suggested that the BrO$_3{}^-$ conversion in a continuous reactor could be increased by either decreasing the liquid flow rate or raising the catalyst loading, meaning increased contact time [48]. The goal of optimizing the contact time is, rather than increasing the already very high (>99%) conversion, to maximize the treatable flow rate of bromate and minimizing the amount of catalyst used while keeping to the 10-ppb guideline. Hence, different feed flow rates (1.8, 3.0, 5.0, and 7.8 mL min^{-1}) and different catalyst loadings (100, 200, 300 mg) were tested, using distilled water containing 200 ppb of bromate. The results obtained using different feed flow rates are presented in Figure 5, and the results obtained using different catalyst loadings are presented in Figure 6.
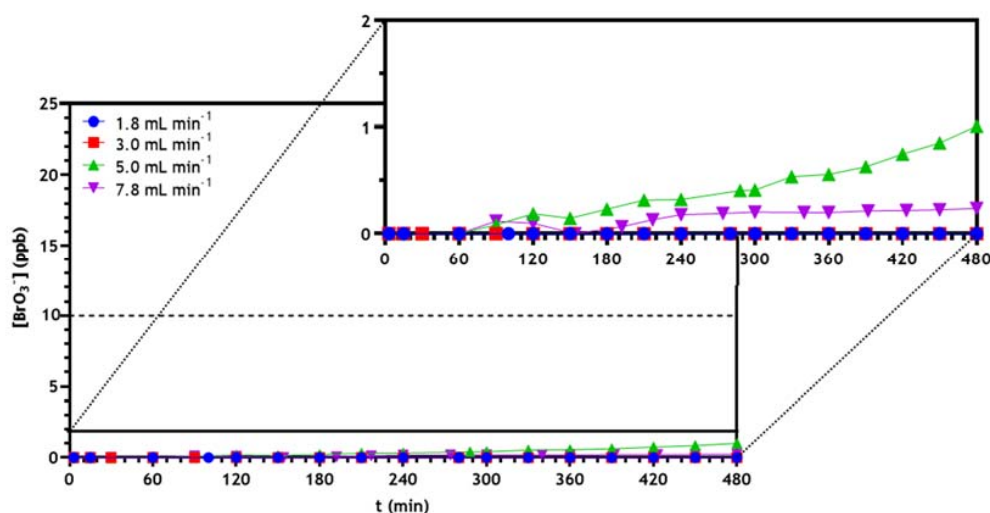
Figure 5. Bromate concentration (ppb) during continuous hydrogen reduction over the catalyst 1 wt.% Pd/MWCNT-O mixed with 0.500 mm carborundum under H_2 using different feed flow rates of water containing bromate. (200 mg_{CAT}, H_2 = 50 cm^3 min^{-1}, C (BrO_3^-) = 200 ppb).
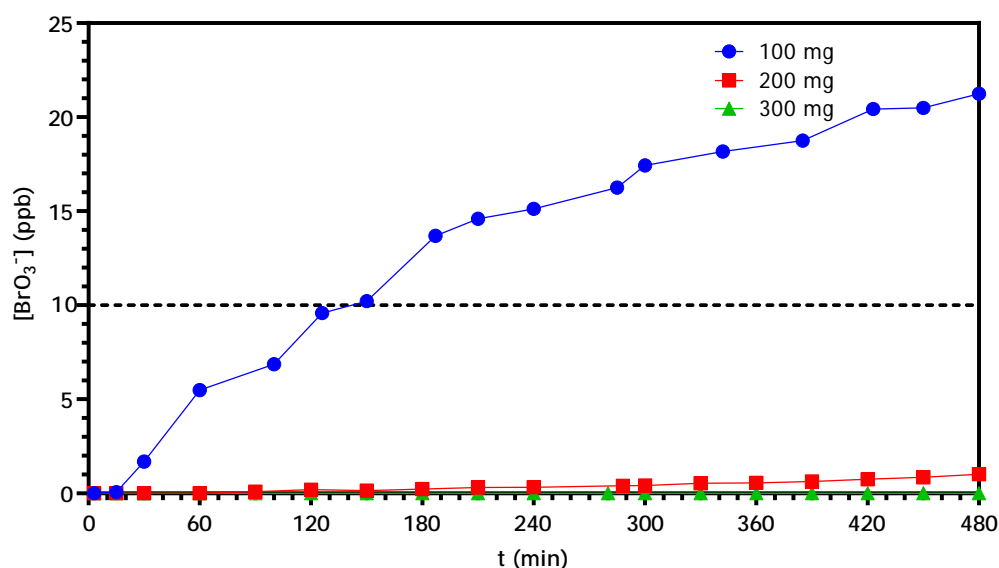

Figure 6. Bromate concentration (ppb) during continuous hydrogen reduction using different catalyst loadings of 1 wt.% Pd/MWCNT-O mixed with 0.500 mm carborundum under H_2. (Q = 5 mL min^{-1}, H_2 = 50 cm^3 min^{-1}, C (BrO_3^-) = 200 ppb).

Every flow rate tested performed very similarly with excellent performances during the 8 h time window for the reaction. An increase in the feed flow rate provides less contact time between the flowing solution and the catalytic bed, but even so, outlet bromate concentrations obtained with 7.8 mL min^{-1} of flow rate were still within the legal guidelines for bromate in drinking water. For flow rates under 3.0 mL min^{-1}, bromate concentrations below detection levels were obtained. These results were expected since these feed rates provided a larger contact time between the solution and the catalytic bed.

From Figure 6 it is evident that while an increase above 200 mg of catalyst does not allow a significant increase in bromate reduction that justifies the use of this much more catalyst and the costs associated with the catalyst synthesis process, less than 200 mg causes considerable performance losses. The bed height was maintained in these experiments, and since the inert filler has a larger diameter, the mean particle size of the bed shifted to higher values with the decrease in catalyst mass. Thus, if the radial dispersion was a concern with the as-received MWCNT support, the use of less catalyst could lead to a similar catalytic

performance as those with higher catalyst content due to the trade-off between the amount of active centers and radial dispersion [42]. However, and since a big drop in activity was seen, it is safe to suggest that the viscous forces are not predominant in the liquid flow through the fixed bed under these conditions. With all this in mind, 12.5 cm^3 min^{-1} of H$_2$, 7.8 mL min^{-1} of flowing solution, and 200 mg of catalyst were considered the optimal conditions for bromate reduction using this system while going forward.

3.2.4. Application to Real Drinking Water

The activity of the Pd nanostructured catalysts for the bromate reduction was also tested in semi-batch and continuous mode using real drinking waters. The water samples were obtained from a well in Coimbra, Portugal, along with water from a WTP in the same region, and their compositions are given in Table 1. When compared with distilled water, these waters have complex matrices, so a decrease in the performance and stability of the catalysts is expected [49]. Initially, semi-batch tests were carried out to evaluate the influence of inorganic as well as organic content on the catalytic reduction process, and since no bromate was found in these waters (due to the seasonal operation of the water treatment plant), a concentrated solution of BrO$_3$$^-$, prepared from NaBrO$_3$ was added to the water matrices, in order to obtain a bromate concentration of 200 ppb. The 1%Pd/MWCNT-BM catalyst was selected as it presented the best catalytic results in the semi-batch reactor system carried out with distilled water (see Section 3.2.1), and Figure 7 shows the obtained results from the catalytic reduction of bromate with hydrogen in the semi-batch reactor system when using these three types of water: distilled water; groundwater from a well; and water from a WTP.
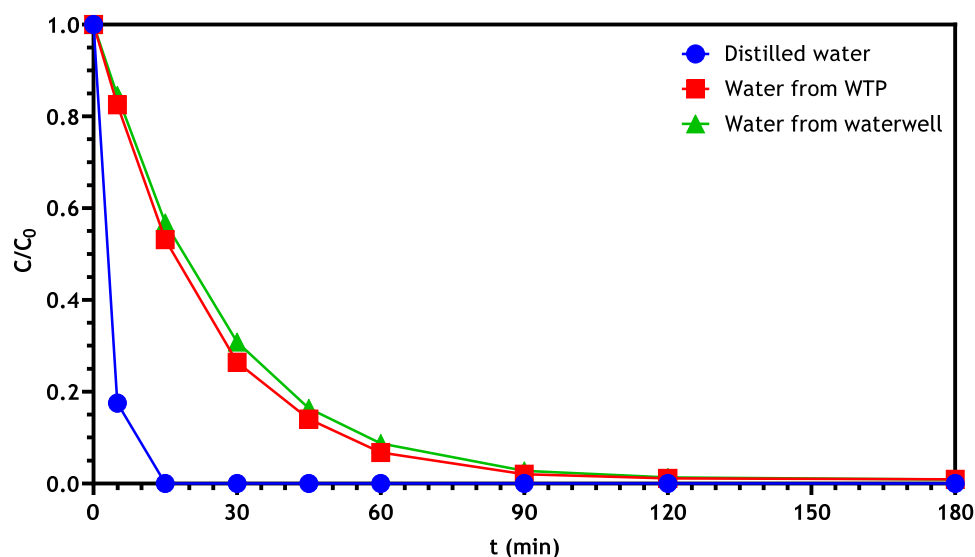

Figure 7. Dimensionless bromate concentration during semi-batch hydrogen reduction over the catalyst 1 wt.% Pd/MWCNT-BM using different types of water. (H$_2$ = 50 cm^3 min^{-1}, C$_0$ (BrO$_3$$^-$) = 200 ppb, 0.125 g$_{CAT}$ L^{-1}).

Both effluents showed a negative influence on the bromate conversion, with small differences between them, depending on the water compositions. It can be observed that the catalytic system went from total conversion in less than 15 min when using distilled water, to only nearly 100% conversion after 2 h of reaction. As can be seen, the presence of other ions and the organic content influence the catalytic activity. The bromate reaction mechanism is an adsorption-controlled reaction process; hence, the presence of different ionic species might trigger a competitive adsorption on the metal actives sites and consequently suppress the bromate reduction [50]. Partial deactivation of the catalyst due to the irreversible adsorption of some ions present, and/or the blocking of active centers by the organic load might also be the reason for a decrease in the catalytic

performance [49]. Zhang et al. [51] reported that anions with high ionic charge and high affinity on Pd causes more noticeable inhibition effects, where the presence of coexisting anions in water compete with bromate for adsorption on the catalyst surface, consequently suppressing the catalytic hydrogenation of bromate. The same was reported by Chen et al. [50] when testing the catalytic reduction of bromate in the presence of Cl^-, SO_4^{2-} and Br^- to assess the impact of co-existing anions. The SO_4^{2-}, compared to Cl^- and Br^-, has a higher ionic charge, resulting in stronger adsorption and thus a more prominent inhibition effect on the bromate reduction. An anion with a high ionic charge and small ionic size invoke a strong electrostatic interaction, and subsequently, is preferentially adsorbed on the positively charged catalyst surface. In addition, increasing the concentration of the coexisting anions leads to enhanced inhibition effects [50,51]. It was also reported that the catalyst deactivation appears more significant when harder waters are treated (high content of Ca^{2+} and Mg^{2+}), resulting in an obstruction of the catalyst by the deposition of calcium salts, making it more difficult to access the catalytic active centers [10]. Regardless, the ball-milled sample clearly demonstrated complete bromate reduction during the whole treatment time from both the water well sample and the WTP sample, although it contained various competing ions. On top of this, in order to test the real possibilities of these catalysts for industrial applications and assess the catalyst performance using real water for a longer duration of reaction time, a continuous catalytic bromate reduction experiment was conducted using water from a WTP in the optimized conditions previously conducted (see Section 3.2.3) for a continuous operation of ~205 flow passages through the catalytic bed. Figure 8 shows bromate concentrations using the MWCNT-O sample in the fixed bed reactor for a continuous operation reaction.
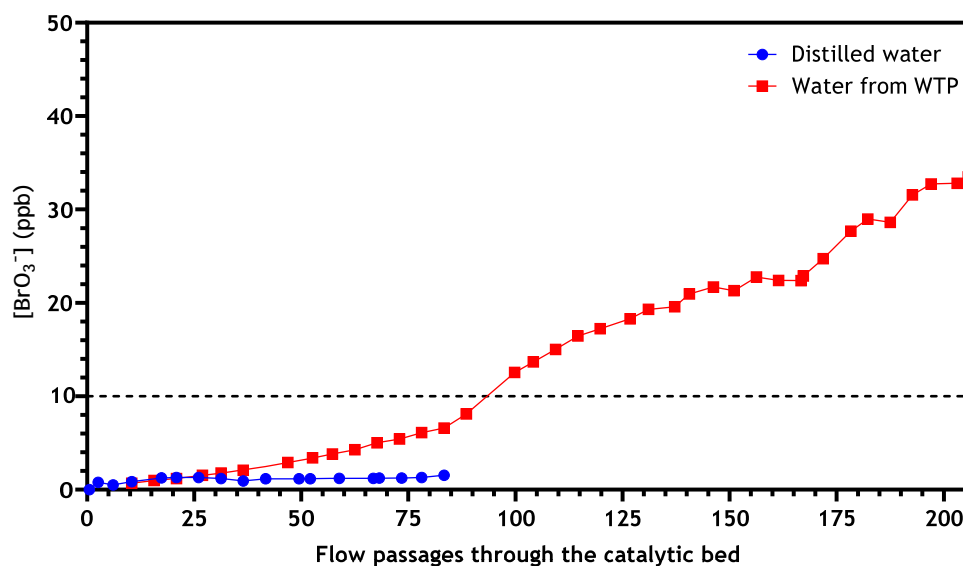

Figure 8. Bromate concentration (ppb) during continuous hydrogen reduction over the catalyst 1 wt.% Pd/MWCNT-O mixed with 0.500 mm carborundum under H_2 using distilled water and water from a water treatment plant. (Q = 7.8 mL min^{-1}, 200 mg_{CAT}, H_2 = 12.5 cm^3 min^{-1}, C (BrO_3^-) = 200 ppb).

Similar to the results found in the semi-batch reactor, a decrease in the performance of the catalyst was observed when using real water. After 83 flow passages through the catalytic bed, bromate conversion rates went from >99% for the distilled water to ~95%. Furthermore, the tendency for the deactivation of the catalyst over time is much more apparent here, where higher bromate concentrations are obtained as the number of passages increases. After ~205 passages through the catalytic bed, a bromate conversion rate of ~83% was obtained. This behavior is consistent with the competitive adsorption model proposed for the deactivation of the catalyst. The experiment with distilled water shows an initial deactivation step likely related to the release of small amounts of Pd, later stabilizing and thus suggesting no further leaching after ~20 flow passage times. On

the other hand, the experiment in WTP water resulted in a constant decrease in activity throughout the >200 flow passages times, suggesting a constant mechanism of deactivation.

Santos et al. [52] verified that the catalytic reduction of NO_3^- in the presence of 1% Pd-1% Cu/CNT catalyst was negatively affected by the presence of a high concentrations of organic matter in solution, being the main reason that led to catalyst deactivation. However, for the experiments conducted in the presence of lower concentrations of organic matter (TOC values around 2 mg L^{-1}), efficient catalytic results were obtained. Furthermore, it was also reported that the catalyst used was active for NO_2^- and BrO_3^- reduction, even in the presence of high organic matter concentrations (with a small loss of efficiency when compared with the same catalyst used for nitrate reduction).

Since the WTP water used in the conducted experiments was found to only have a TOC value of 3.7 mg L^{-1}, it is safe to assume that the catalyst deactivation is mainly related to the competitive adsorption of co-existing ions or the formation of mineral deposits on the catalyst active centers, with only small compromises related to the presence of organic matter and the dissolution of Pd. Further studies are required with this catalytic system to design an efficient regeneration system, provided the deactivation mechanism can be further understood. Natural organic matter has been removed from metallic catalysts in similar systems using a base [53], and the inorganic matter has been shown to be efficiently removed by washing with hypochlorite [54].

4. Conclusions

A systematic study was carried out to assess the role of the properties of nanostructured carbon supports in the performance of a catalytic system for the reduction of bromate over palladium. It has been observed that it is possible to reduce bromate in water with hydrogen using both semi-batch and continuous operation modes, but the chemical and textural properties of the supports have been shown to significantly affect the performance of the catalysts. In semi-batch experiments, the following trend for the catalyst supports was found: oxidative treatment < original < nitrogen-doped < milling process. In the continuous fixed bed reactor, all catalysts tested proved to be active in the reduction of bromate under hydrogen, and although possessing greater intrinsic catalytic activity, the smaller particles of mechanically modified carbon nanotubes hampered its performance in the fixed bed reactor, where catalyst dilution with inert particles allowed for better radial dispersion, immensely improving the performance of the reactor. A decrease in the catalytic performance for the real waters tested was observed, which was attributed to the blocking of active centers by the organic load and the competitive adsorption of the different ions on the active centers of the catalyst. A tendency for a deactivation of the catalyst over time was also apparent, where a constant decrease in activity throughout the 200 flow passage times is seen, likely related to the competitive adsorption of inorganic matter on the catalyst active centers or formation of mineral deposits on the catalyst active centers.

Institutional Review Board Statement: Not applicable.

Informed Consent Statement: Not applicable.

Conflicts of Interest: The authors declare no conflict of interest.

References

1. World Health Organization. *Guidelines for Drinking-Water Quality: Fourth Edition Incorporating First Addendum*, 4th ed.; World Health Organization: Switzerland, Geneva, 2017.
2. Butler, R.A.Y.; Godley, A.; Lytton, L.; Cartmell, E. Bromate Environmental Contamination: Review of Impact and Possible Treatment. *Crit. Rev. Environ. Sci. Technol.* **2005**, *35*, 193–217. [CrossRef]
3. Huang, W.-J.; Cheng, Y.-L. Effect of characteristics of activated carbon on removal of bromate. *Sep. Purif. Technol.* **2008**, *59*, 101–107. [CrossRef]
4. Huang, X.; Wang, L.; Zhou, J.; Gao, N. Photocatalytic decomposition of bromate ion by the UV/P25-Graphene processes. *Water Res.* **2014**, *57*, 1–7. [CrossRef] [PubMed]
5. Wiśniewski, J.A.; Kabsch-Korbutowicz, M.; Łakomska, S. Removal of bromate ions from water in the processes with ion-exchange membranes. *Sep. Purif. Technol.* **2015**, *145*, 75–82. [CrossRef]
6. Kishimoto, N.; Matsuda, N. Bromate Ion Removal by Electrochemical Reduction Using an Activated Carbon Felt Electrode. *Environ. Sci. Technol.* **2009**, *43*, 2054–2059. [CrossRef] [PubMed]
7. Restivo, J.; Soares, O.S.G.P.; Órfão, J.J.M.; Pereira, M.F.R. Metal assessment for the catalytic reduction of bromate in water under hydrogen. *Chem. Eng. J.* **2015**, *263*, 119–126. [CrossRef]
8. Perez-Coronado, A.M.; Soares, O.S.G.P.; Calvo, L.; Rodriguez, J.J.; Gilarranz, M.A.; Pereira, M.F.R. Catalytic reduction of bromate over catalysts based on Pd nanoparticles synthesized via water-in-oil microemulsion. *Appl. Catal. B Environ.* **2018**, *237*, 206–213. [CrossRef]
9. Soares, O.S.G.P.; Ramalho, P.S.F.; Fernandes, A.; Órfão, J.J.M.; Pereira, M.F.R. Catalytic bromate reduction in water: Influence of carbon support. *J. Environ. Chem. Eng.* **2019**, *7*, 103015–103023. [CrossRef]
10. Cerrillo, J.L.; Palomares, A.E. A Review on the Catalytic Hydrogenation of Bromate in Water Phase. *Catalysts* **2021**, *11*, 365. [CrossRef]
11. Cerrillo, J.L.; Lopes, C.W.; Rey, F.; Palomares, A.E. The Influence of the Support Nature and the Metal Precursor in the Activity of Pd-based Catalysts for the Bromate Reduction Reaction. *ChemCatChem* **2021**, *13*, 1230–1238. [CrossRef]
12. Soares, O.S.G.P.; Gonçalves, A.G.; Delgado, J.J.; Órfão, J.J.M.; Pereira, M.F.R. Modification of carbon nanotubes by ball-milling to be used as ozonation catalysts. *Catal. Today* **2015**, *249*, 199–203. [CrossRef]
13. Morais, D.F.S.; Boaventura, R.A.R.; Moreira, F.C.; Vilar, V.J.P. Bromate removal from water intended for human consumption by heterogeneous photocatalysis: Effect of major dissolved water constituents. *Chemosphere* **2021**, *263*, 128111–128119. [CrossRef] [PubMed]
14. Wu, Z.; Tang, Y.; Yuan, X.; Qiang, Z. Reduction of bromate by zero valent iron (ZVI) enhances formation of brominated disinfection by-products during chlorination. *Chemosphere* **2021**, *268*, 129340–129347. [CrossRef]
15. Chen, X.; Huo, X.; Liu, J.; Wang, Y.; Werth, C.J.; Strathmann, T.J. Exploring beyond palladium: Catalytic reduction of aqueous oxyanion pollutants with alternative platinum group metals and new mechanistic implications. *Chem. Eng. J.* **2017**, *313*, 745–752. [CrossRef]
16. Restivo, J.; Soares, O.S.G.P.; Órfão, J.J.M.; Pereira, M.F.R. Catalytic reduction of bromate over monometallic catalysts on different powder and structured supports. *Chem. Eng. J.* **2017**, *309*, 197–205. [CrossRef]
17. Palomares, A.E.; Franch, C.; Yuranova, T.; Kiwi-Minsker, L.; García-Bordeje, E.; Derrouiche, S. The use of Pd catalysts on carbon-based structured materials for the catalytic hydrogenation of bromates in different types of water. *Appl. Catal. B Environ.* **2014**, *146*, 186–191. [CrossRef]
18. Marco, Y.; García-Bordejé, E.; Franch, C.; Palomares, A.E.; Yuranova, T.; Kiwi-Minsker, L. Bromate catalytic reduction in continuous mode using metal catalysts supported on monoliths coated with carbon nanofibers. *Chem. Eng. J.* **2013**, *230*, 605–611. [CrossRef]
19. Thakur, D.B.; Tiggelaar, R.M.; Gardeniers, J.G.E.; Lefferts, L.; Seshan, K. Silicon based microreactors for catalytic reduction in aqueous phase: Use of carbon nanofiber supported palladium catalyst. *Chem. Eng. J.* **2013**, *227*, 128–136. [CrossRef]
20. Höller, V.; Yuranov, I.; Kiwi-Minsker, L.; Renken, A. Structured multiphase reactors based on fibrous catalysts: Nitrite hydrogenation as a case study. *Catal. Today* **2001**, *69*, 175–181. [CrossRef]
21. Palomares, A.E.; Franch, C.; Corma, A. A study of different supports for the catalytic reduction of nitrates from natural water with a continuous reactor. *Catal. Today* **2011**, *172*, 90–94. [CrossRef]
22. Yuranova, T.; Franch, C.; Palomares, A.E.; Garcia-Bordejé, E.; Kiwi-Minsker, L. Structured fibrous carbon-based catalysts for continuous nitrate removal from natural water. *Appl. Catal. B Environ.* **2012**, *123*, 221–228. [CrossRef]
23. Gonçalves, A.G.; Figueiredo, J.L.; Órfão, J.J.M.; Pereira, M.F.R. Influence of the surface chemistry of multi-walled carbon nanotubes on their activity as ozonation catalysts. *Carbon* **2010**, *48*, 4369–4381. [CrossRef]
24. Soares, S.; Rocha, R.P.; Gonçalves, A.; Figueiredo, J.; Órfão, J.; Pereira, F. Easy method to prepare N-doped carbon nanotubes by ball milling. *Carbon* **2015**, *91*, 114–121. [CrossRef]

25. Soares, O.S.G.P.; Rocha, R.P.; Órfão, J.J.M.; Pereira, M.F.R.; Figueiredo, J.L. Mechanothermal Approach for N-, S-, P-, and B-Doping of Carbon Nanotubes: Methodology and Catalytic Performance in Wet Air Oxidation. *C—J. Carbon Res.* **2019**, *5*, 30. [CrossRef]

26. Birch, M.E.; Ruda-Eberenz, T.A.; Chai, M.; Andrews, R.; Hatfield, R.L. Properties that Influence the Specific Surface Areas of Carbon Nanotubes and Nanofibers. *Ann. Occup. Hyg.* **2013**, *57*, 1148–1166. [PubMed]

27. Rocha, R.P.; Soares, O.S.G.P.; Gonçalves, A.G.; Órfão, J.J.M.; Pereira, M.F.R.; Figueiredo, J.L. Different methodologies for synthesis of nitrogen doped carbon nanotubes and their use in catalytic wet air oxidation. *Appl. Catal. A Gen.* **2017**, *548*, 62–70. [CrossRef]

28. Rocha, R.P.; Sousa, J.P.S.; Silva, A.M.T.; Pereira, M.F.R.; Figueiredo, J.L. Catalytic activity and stability of multiwalled carbon nanotubes in catalytic wet air oxidation of oxalic acid: The role of the basic nature induced by the surface chemistry. *Appl. Catal. B Environ.* **2011**, *104*, 330–336. [CrossRef]

29. Zhang, J.; Zou, H.; Qing, Q.; Yang, Y.; Li, Q.; Liu, Z.; Guo, X.; Du, Z. Effect of Chemical Oxidation on the Structure of Single-Walled Carbon Nanotubes. *J. Phys. Chem. B* **2003**, *107*, 3712–3718. [CrossRef]

30. Hu, H.; Zhao, B.; Itkis, M.E.; Haddon, R.C. Nitric Acid Purification of Single-Walled Carbon Nanotubes. *J. Phys. Chem. B* **2003**, *107*, 13838–13842. [CrossRef]

31. Soares, O.S.G.P.; Órfão, J.J.M.; Pereira, M.F.R. Nitrate Reduction Catalyzed by Pd–Cu and Pt–Cu Supported on Different Carbon Materials. *Catal. Lett.* **2010**, *139*, 97–104. [CrossRef]

32. Kasaini, H.; Goto, M.; Furusaki, S. Selective Separation of Pd(II), Rh(III), and Ru(III) Ions from a Mixed Chloride Solution Using Activated Carbon Pellets. *Sep. Sci. Technol.* **2000**, *35*, 1307–1327. [CrossRef]

33. Watanabe, S.; Arunajatesan, V. Influence of Acid Modification on Selective Phenol Hydrogenation Over Pd/Activated Carbon Catalysts. *Top. Catal.* **2010**, *53*, 1150–1152. [CrossRef]

34. Contreras, R.C.; Guicheret, B.; Machado, B.F.; Rivera-Cárcamo, C.; Alvarez, M.A.C.; Salas, B.V.; Ruttert, M.; Placke, T.; Réguillon, A.F.; Vanoye, L.; et al. Effect of mesoporous carbon support nature and pretreatments on palladium loading, dispersion and apparent catalytic activity in hydrogenation of myrcene. *J. Catal.* **2019**, *372*, 226–244. [CrossRef]

35. Simonov, P.A.; Troitskii, S.Y.; Likholobov, V.A. Preparation of the Pd/C catalysts: A molecular-level study of active site formation. *Kinet. Catal.* **2000**, *41*, 255–269. [CrossRef]

36. Rao, R.G.; Blume, R.; Hansen, T.W.; Fuentes, E.; Dreyer, K.; Moldovan, S.; Ersen, O.; Hibbitts, D.D.; Chabal, Y.J.; Schlögl, R.; et al. Interfacial charge distributions in carbon-supported palladium catalysts. *Nat. Commun.* **2017**, *8*, 340. [CrossRef] [PubMed]

37. Krishna Kumar, M.; Ramaprabhu, S. Palladium dispersed multiwalled carbon nanotube based hydrogen sensor for fuel cell applications. *Int. J. Hydrog. Energy* **2007**, *32*, 2518–2526. [CrossRef]

38. Santos, A.S.G.G.; Restivo, J.; Orge, C.A.; Pereira, M.F.R.; Soares, O.S.G.P. Nitrate Catalytic Reduction over Bimetallic Catalysts: Catalyst Optimization. *C—J. Carbon Res.* **2020**, *6*, 78. [CrossRef]

39. Solhy, A.; Machado, B.F.; Beausoleil, J.; Kihn, Y.; Gonçalves, F.; Pereira, M.F.R.; Órfão, J.J.M.; Figueiredo, J.L.; Faria, J.L.; Serp, P. MWCNT activation and its influence on the catalytic performance of Pt/MWCNT catalysts for selective hydrogenation. *Carbon* **2008**, *46*, 1194–1207. [CrossRef]

40. Soares, O.S.G.P.; Rocha, R.P.; Gonçalves, A.G.; Figueiredo, J.L.; Órfão, J.J.M.; Pereira, M.F.R. Highly active N-doped carbon nanotubes prepared by an easy ball milling method for advanced oxidation processes. *Appl. Catal. B Environ.* **2016**, *192*, 296–303. [CrossRef]

41. Yuranova, T.; Kiwi-Minsker, L.; Franch, C.; Palomares, A.E.; Armenise, S.; García-Bordejé, E. Nanostructured Catalysts for the Continuous Reduction of Nitrates and Bromates in Water. *Ind. Eng. Chem. Res.* **2013**, *52*, 13930–13937. [CrossRef]

42. Alsolami, B.H.; Berger, R.J.; Makkee, M.; Moulijn, J.A. Catalyst Performance Testing in Multiphase Systems: Implications of Using Small Catalyst Particles in Hydrodesulfurization. *Ind. Eng. Chem. Res.* **2013**, *52*, 9069–9085. [CrossRef]

43. Yaseneva, P.; Marti, C.F.; Palomares, E.; Fan, X.; Morgan, T.; Perez, P.S.; Ronning, M.; Huang, F.; Yuranova, T.; Kiwi-Minsker, L.; et al. Efficient reduction of bromates using carbon nanofibre supported catalysts: Experimental and a comparative life cycle assessment study. *Chem. Eng. J.* **2014**, *248*, 230–241. [CrossRef]

44. Gašparovičová, D.; Králik, M.; Hronec, M.; Vallušová, Z.; Vinek, H.; Corain, B. Supported Pd–Cu catalysts in the water phase reduction of nitrates: Functional resin versus alumina. *J. Mol. Catal. A Chem.* **2007**, *264*, 93–102. [CrossRef]

45. Pintar, A.; Batista, J. Catalytic hydrogenation of aqueous nitrate solutions in fixed-bed reactors. *Catal. Today* **1999**, *53*, 35–50. [CrossRef]

46. Durkin, D.P.; Ye, T.; Choi, J.; Livi, K.J.T.; Long, H.C.D.; Trulove, P.C.; Fairbrother, D.H.; Haverhals, L.M.; Shuai, D. Sustainable and scalable natural fiber welded palladium-indium catalysts for nitrate reduction. *Appl. Catal. B Environ.* **2018**, *221*, 290–301. [CrossRef]

47. Soares, O.S.G.P.; Órfão, J.J.M.; Ruiz-Martínez, J.; Silvestre-Albero, J.; Sepúlveda-Escribano, A.; Pereira, M.F.R. Pd–Cu/AC and Pt–Cu/AC catalysts for nitrate reduction with hydrogen: Influence of calcination and reduction temperatures. *Chem. Eng. J.* **2010**, *165*, 78–88. [CrossRef]

48. Stylianou, M.A.; Inglezakis, V.J.; Moustakas, K.G.; Malamis, S.P.; Loizidou, M.D. Removal of Cu(II) in fixed bed and batch reactors using natural zeolite and exfoliated vermiculite as adsorbents. *Desalination* **2007**, *215*, 133–142. [CrossRef]

49. Soares, O.S.G.P.; Órfão, J.J.M.; Gallegos-Suarez, E.; Castillejos, E.; Rodríguez-Ramos, I.; Pereira, M.F.R. Nitrate reduction over a Pd-Cu/MWCNT catalyst: Application to a polluted groundwater. *Environ. Technol.* **2012**, *33*, 2353–2358. [CrossRef]

50. Chen, H.; Xu, Z.; Wan, H.; Zheng, J.; Yin, D.; Zheng, S. Aqueous bromate reduction by catalytic hydrogenation over Pd/Al2O3 catalysts. *Appl. Catal. B Environ.* **2010**, *96*, 307–313. [CrossRef]

51. Zhang, P.; Jiang, F.; Chen, H. Enhanced catalytic hydrogenation of aqueous bromate over Pd/mesoporous carbon nitride. *Chem. Eng. J.* **2013**, *234*, 195–202. [CrossRef]

52. Santos, A.S.G.G.; Restivo, J.; Orge, C.A.; Pereira, M.F.R.; Soares, O.S.G.P. Influence of organic matter formed during oxidative processes in the catalytic reduction of nitrate. *J. Environ. Chem. Eng.* **2021**, *9*, 105545–105556. [CrossRef]

53. Chaplin, B.P.; Roundy, E.; Guy, K.A.; Shapley, J.R.; Werth, C.J. Effects of Natural Water Ions and Humic Acid on Catalytic Nitrate Reduction Kinetics Using an Alumina Supported Pd−Cu Catalyst. *Environ. Sci. Technol.* **2006**, *40*, 3075–3081. [CrossRef] [PubMed]

54. Chaplin, B.P.; Shapley, J.R.; Werth, C.J. Regeneration of Sulfur-Fouled Bimetallic Pd-Based Catalysts. *Environ. Sci. Technol.* **2007**, *41*, 5491–5497. [CrossRef] [PubMed]